Pergamon

Cement and Concrete Research 32 (2002) 1199–1206

CEMENT AND CONCRETE RESEARCH

Alkali–silica reaction
A method to quantify the reaction degree

D. Bulteel[a,*], E. Garcia-Diaz[a], C. Vernet[b], H. Zanni[c]

[a]*Département de génie civil de l'Ecole Nationale Supérieure des Techniques Industrielles et des Mines de Douai, 941 rue Charles Bourseul, 838-59508 Douai Cedex B.P., France*

[b]*Laboratoire central de recherche du groupe Lafarge, Saint Quentin Fallavier, France*

[c]*Laboratoire de physique et mécanique des milieux hétérogènes de l'Ecole Supérieure de Physique et Chimie Industrielle de Paris, Paris, France*

Received 30 April 2001; accepted 4 February 2002

Abstract

We propose a new chemical method for quantitative measurement of the reaction degrees of the alkali–silica reaction (ASR). We apply this method to a crushed natural reactive aggregate kept in contact with an alkaline solution, lime saturated by an appropriate amount of portlandite. This chemical system is designed to model the concrete capillary pores alkaline solution, in contact with reactive aggregates. Two reaction steps are taken into account in the mechanism: formation of Q_3 sites made by breaking up siloxane bonds of the reactive silica and dissolution of these Q_3 sites. The dissolution degree is measured by a selective acid treatment, and the nature of silica into solution is characterised by liquid NMR spectroscopy. The remaining silica is composed of Q_4 tetrahedrons and Q_3 protonated sites identified by solid NMR spectroscopy. These Q_3 protonated sites are measured by thermogravimetry analysis. We show that the formation Q_3 sites prevails on dissolution as the reaction progresses and contributes to an internal silica gel generation. The limiting step is the siloxane breaking up. Petrographic observations show that the reaction front penetrates in the aggregate through its porosity.

Keywords: Kinetics; Alkali–aggregate reaction; Aggregate; Reaction degree

1. Introduction

Research on alkali–silica reaction (ASR) was often focused on the silica-rich gels formed between reactive siliceous aggregates, $Ca(OH)_2$ and alkali salts, in relation with concrete expansion. Many accelerated tests were developed, and many works were done on ASR diagnosis:

- the ultraviolet fluorescence of gels where calcium or alkalis have been exchanged with uranyl ions allows to identify the ASR gel [1],
- petrographic and electron microscope examinations allow to identify the reactive minerals, the altered aggregates and the reaction products [2] and
- the mineralogical analysis of concrete with the determination of the soluble silica can give information on the ASR occurrence [3].

However, these diagnosis methods of ASR are generally not quantitative. Moreover, the specific identification of ASR in structures is often difficult, because of the simultaneous occurrence of different causes of expansion. Therefore, the "potential of remaining expansion" tests on concrete cores [4] could be biased by other swelling processes like delayed ettringite formation (DEF).

To develop a diagnosis technique being both specific and quantitative, we try to relate expansion to the reaction degree, more than to the reaction products properties. First, we have to develop a chemical method to measure the reaction degree. We use a chemical concrete subsystem, involving the main ASR reagents: ground aggregate, $Ca(OH)_2$ and KOH. These reagents, which are kept in contact in a closed vessel at given temperatures and pressures, can be considered on a kinetic point of view like a "model reactor" representative of the

* Corresponding author. Tel.: +33-3-27-71-24-21; fax: +33-3-27-71-29-16.

E-mail address: bulteel@ensm-douai.fr (D. Bulteel).

0008-8846/02/$ – see front matter
PII: S0008-8846(02)00759-7

chemistry of reactive aggregates in contact with the concrete capillary pores alkaline solution. This model reactor allows an accurate determination of the reaction kinetics described by the evolutions of both solid and liquid phases.

We describe thereafter:

- the assumptions made on the two ASR kinetics steps taken in consideration,
- the definition of the reaction degrees,
- the studied aggregate type and composition,
- the model reactor technique,
- the liquid phase evolution and silica polymerisation degree and
- the solid phase evolution in terms of structural aspects.

2. Chemical mechanisms of alkali aggregate reaction

The ASR mechanism was described using different models [5–9] and can be written following two main steps:

2.1. Formation of Q3 sites (Step 1) due to a first siloxane bonds breaking up by hydroxide ions attack

$$2SiO_2 + OH^- \rightarrow SiO_{5/2}^- + SiO_{5/2}H \quad (1)$$

Here, on a structural point of view, SiO_2 represents Q_4 silicon tetrahedron sharing four oxygens with four neighbours, and using a simplified notation, $SiO_{5/2}^-$ represents the Q_3 (so-called "silanol" sites) negatively charged in a basic solution.

The neutralisation of these Q_3 sites follows the equilibrium (Eq. (2)):

$$SiO_{5/2}H + OH^- \Longleftrightarrow SiO_{5/2}^- + H_2O \quad (2)$$

In contact with an alkaline solution, the preponderant form is $SiO_{5/2}^-$. The Q_3 sites negatively charged are counterbalanced by K^+ and Ca^{2+} cations (Eqs. (3) and (3 bis)):

$$SiO_{5/2}^- + K^+ \rightarrow SiO_{5/2}K \quad (3)$$

$$2SiO_{5/2}^- + Ca^{2+} \rightarrow SiO_{5/2}CaSiO_{5/2} \quad (3\text{ bis})$$

2.2. Dissolution of silica (Step 2) due to continued hydroxide ions attack on the Q_3 sites to form silica ions

$$SiO_{5/2}^- + OH^- + \frac{1}{2}H_2O \rightarrow H_2SiO_4^{2-} \quad (4)$$

These silica ions respects the Iler equilibrium (Eq. (5)):

$$H_2SiO_4^{2-} + H_2O \Longleftrightarrow H_3SiO_4^- + OH^- \quad (5)$$

Afterwards, precipitation of silica ions by the cations of the pore solution of concrete is liable to the formation of C-S-H and/or C-K-S-H phases (Eqs. (6) and (7)):

$$xH_2SiO_4^{2-} + zH_3SiO_4^- + \left(x + \frac{z}{2}\right)Ca^{2+} + wH_2O \rightarrow CaO_{\left(x+\frac{z}{2}\right)}SiO_{2(x+z)}H_2O_{\left(x+\frac{3}{2}z+w\right)} \quad (6)$$

$$xH_2SiO_4^{2-} + zH_3SiO_4^- + \left(x + \frac{z}{2} - \frac{y}{2}\right)Ca^{2+} + yK^+ + wH_2O \rightarrow CaO_{\left(x+\frac{z}{2}-\frac{y}{2}\right)}K_2O_{\frac{y}{2}}SiO_{2(x+z)} \times H_2O_{\left(x+\frac{3}{2}z+w\right)} \quad (7)$$

The Q_3 site formation and the silica dissolution are controlled by the hydroxide diffusivity in reactive grains and by hydroxide absorption on the solid surface. The hydroxide diffusivity increases with the pH and the ionic strength of the solution [10]. At a constant pH and ionic strength, the hydroxide sorption decreases with the increasing size of the hydrated cation [10]. A part of the alkali hydroxide of the concrete pore solution cannot contribute to ASR [11]:

- Alkali hydroxide could induce gypsum dissolution to form portlandite and soluble alkali sulphate. This reaction raises the sulphate concentration of the solution instead of the hydroxide concentration.
- A partial drying of the concrete decreases, more than increases, the alkali hydroxide concentration in pore solution. At modest RH values, the solid network fixes a part of the soluble alkalis.

The diffusion of the silica ions out of the reactive grains is controlled by the Ca^{2+} concentration near the solid–liquid interface. A high concentration favours the precipitation phenomena and limits the silica ion diffusion [10].

Helmuth and Stark [12] describe the precipitated product as a mixture of two end-member phases of well-defined composition: an alkali silicate hydrate and a calcium alkali silicate hydrate. On the other hand, Lombardi et al. [13] consider the precipitates as a continuous series defined by its CaO/SiO_2 molar ratio. These gels present an optimum of stability for a CaO/SiO_2 molar ratio near 0.48 [14]. According to Diamond [15], if the Helmuth and Stark model gives generally meaningful results, further investigations are needed to describe the precipitation products composition.

Generally, the alkali silicate hydrate are considered responsible for the swelling [5–8]. Wieker et al. [16,17] have synthesised a crystalline sodium silicate hydrate called "kanemite" ($Na(HSi_2O_5)\cdot 3H_2O$) thanks to a reaction between $\delta Na_2Si_2O_5$- and SiO_2-containing minerals. The kanemite formation is expansive. Nevertheless, Thomas [18] and Kawamura et al. [19,20] consider that calcium is necessary

to form expansive ASR gels. Perruchot et al. [14] have demonstrated that the formation of ASR gel rich in calcium provokes a positive variation of the total volume of the reactional system under constant pressure.

3. Determination of reaction degrees

The development of our new chemical method to quantify ASR is based on the measurement of the reaction degrees of Steps (1) and (2), which are defined as follows:

- Q_3 sites content:

$$n = \frac{\text{moles of } Q_3 \text{ sites}}{\text{moles of initial silica}} \quad (8)$$

- dissolution degree:

$$\alpha = \frac{\text{moles of dissolved silica}}{\text{moles of initial silica}} \quad (9)$$

From n and α, we can calculate n^*:

$$n^* = \frac{\text{moles of } Q_3 \text{ sites}}{\text{moles of residual silica}} = \frac{n}{1-\alpha} \quad (10)$$

4. The aggregate

The material used is a flint aggregate from north of France. This aggregate is ground to obtain a [0.16–0.63 mm] size distribution. The X-ray fluorescence examination gives a composition close to 99% SiO_2 (Table 1).

The flint crystal lattice has been characterised by crossed polarisation ^{29}Si solid NMR spectroscopy (Fig. 1). This lattice is comprised of SiO_2 Q_4 tetrahedra (peak at –108 ppm) and Q_3 $SiO_{5/2}H$ "silanol" tetrahedra (peak at −99 ppm). The Q_3 mole fraction measured by thermogravimetry was close to 0.07.

The material has a specific area of 0.97 m^2/g and a specific porosity of 3×10^{-3} cm^3/g characterised by BET and BJH analysis. As the external surface calculated, thanks to size distribution, is as low as 0.008 m^2/g, we can conclude that the reactive sites of the studied aggregate are mainly located in some kind of an "internal surface".

Table 1
Composition of the aggregate obtained by X-ray fluorescence analysis

Element	%
SiO_2	99.1
Fe_2O_3	0.4
CaO	0.3
Al_2O_3	0.2

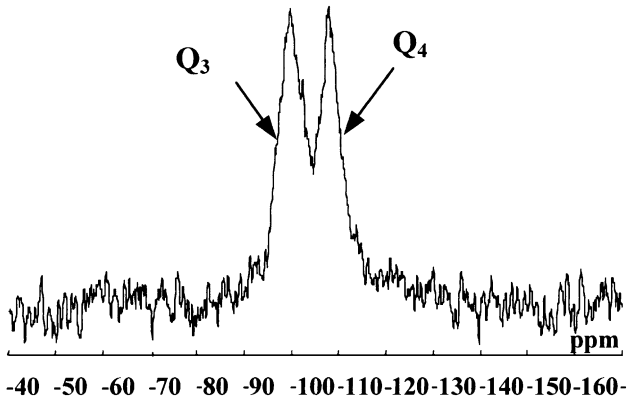

Fig. 1. Crossed polarised ^{29}Si solid NMR spectrum of the flint aggregate.

5. Description of the model reactor

Our model reactor method is based on a part of the AFNOR P18-589 standard [21]. It allows the determination of reaction degrees, obtained by solid and liquid characterisation at different reaction times, and uses the following protocol organised in three stages (Fig. 2).

5.1. Initial stage

A mix of 1 g of crushed aggregate and 0.5 g $Ca(OH)_2$ is introduced in a closed stainless-steel container. After 30 min of preheating, 10 ml KOH solution of a 0.79-M concentration is added. The container is then autoclaved during a given time at 80 °C to accelerate ASR under controlled temperature.

5.2. Stage 1

After the reaction, the aggregate is constituted by Q_4 tetrahedrons that did not react (sound silica) and by the Q_3 tetrahedrons ($SiO_{5/2}K$, $SiO_{5/2}Ca$ $SiO_{5/2}$ and $SiO_{5/2}H$), which constitute the altered silica. In this stage, a large part of the alkaline solution is extracted for ICP and ^{29}Si RMN analyses.

5.3. Stage 2

Thanks to an selective acid treatment using a 250-ml cold 0.5 M HCl solution the C-S-H, C-K-S-H and $Ca(OH)_2$ phases are removed. During this chemical treatment, the Q_3 tetrahedrons $SiO_{5/2}K$ and $SiO_{5/2}CaSiO_{5/2}$ are protonated to form silanols $SiO_{5/2}H$ with a release of K^+ and Ca^{2+} cations. As recommended by the "soluble silica" method

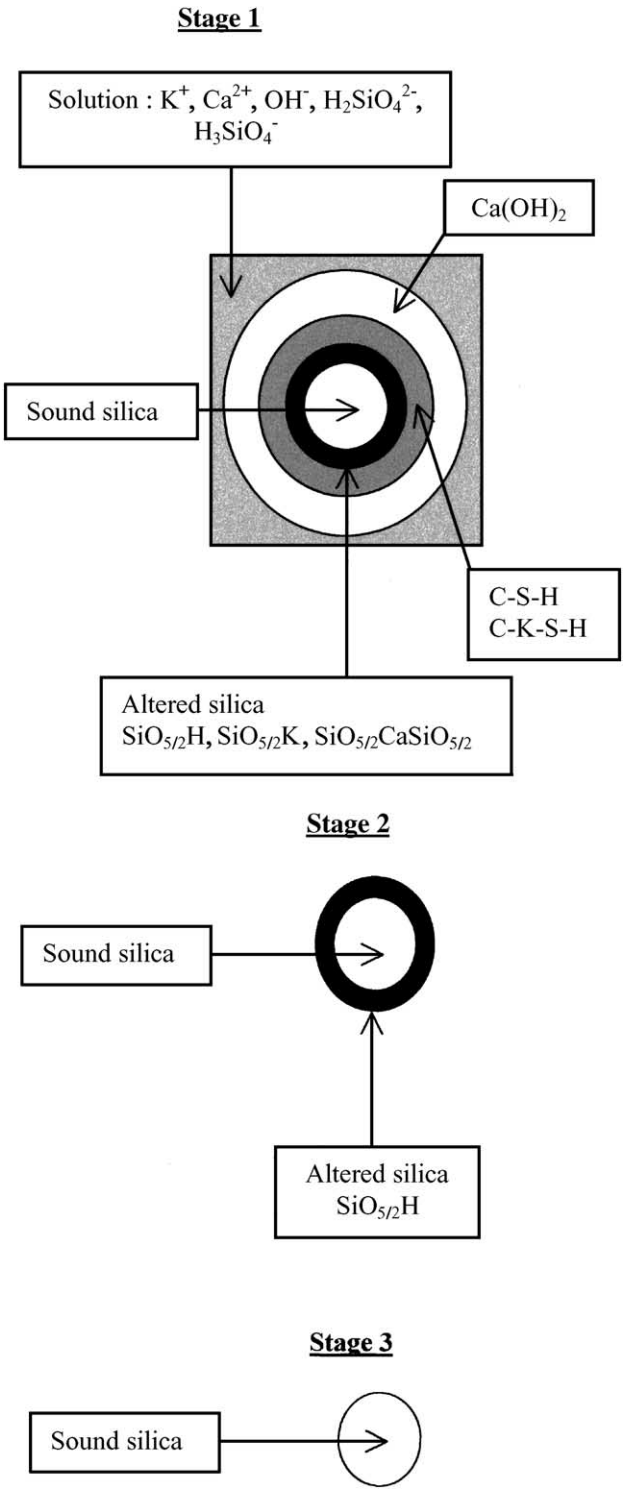

Fig. 2. A schematic presentation of the model reactor.

developed by the LCPC to prevent the silica gel precipitation during the acid attack [22]:

- we used a cold solution and a great liquid solid ratio (250 ml of solution for 1.5 g of initial solid), and

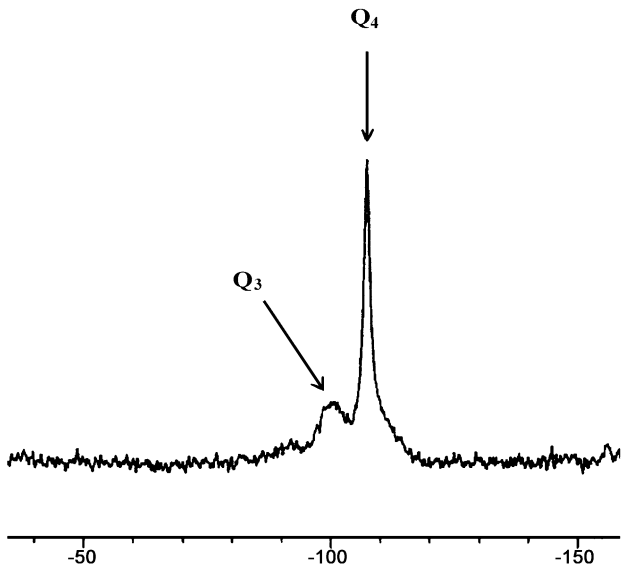

Fig. 3. Single-pulse ^{29}Si solid NMR spectrum of the solid after the acid attack (14 h of reaction at 80 °C).

- we controlled the pH, which must be inferior to one unit during the chemical treatment.

The efficiency of the acid attack is controlled by X-ray fluorescence: The SiO_2 content of the remaining solid must be at least 99%. The remaining solid characterised by ^{29}Si solid NMR spectroscopy (Fig. 3) is composed of residual SiO_2 Q_4 tetrahedra (peak at −108 ppm) and $SiO_{5/2}H$ Q_3 tetrahedra (peak at −101 ppm). These ^{29}Si solid NMR spectra confirm the absence of silica gel precipitation during the acid treatment: We do not observe a widening of the single sharp line of the Q_4 network.

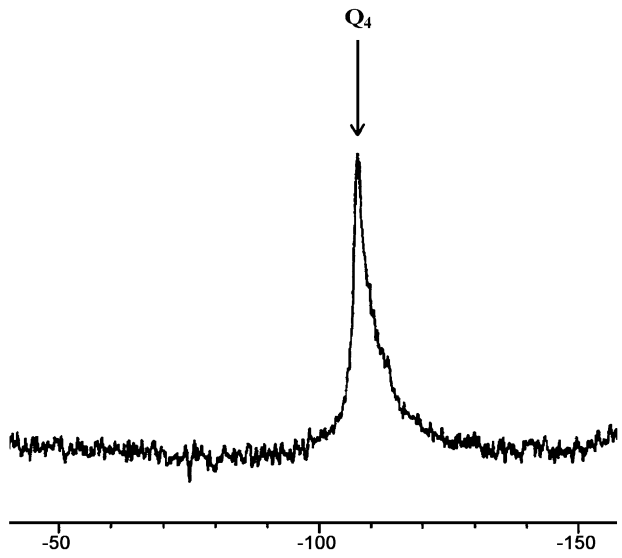

Fig. 4. Single-pulse ^{29}Si solid NMR spectrum of the solid after the thermal treatment (14 h of reaction at 80 °C).

5.4. Stage 3

After a thermal treatment of the residual solid at 1000 °C, the silanol groups are condensed to give back silica Q_4 and release water following (Eq. (11)):

$$2SiO_{5/2}H \xrightarrow{1000^{\circ}C} 2SiO_2 + H_2O \quad (11)$$

These Q_4 tetrahedra have been identified by ^{29}Si solid NMR spectroscopy (Fig. 4). The water release measurement by thermogravimetry allows the calculation of the quantity of Q_3 tetrahedra in the aggregate sample (variable n defined in Eq. (8)). The weight of the residual silica allows to determine by difference the quantity of dissolved silica (variable α defined in Eq. (9)).

6. Results and discussion

6.1. The reaction degrees

6.1.1. Evolution of α

The dissolution degree α according to time is given in Fig. 5. After a short plateau, about 6 h long, α increases to reach an asymptotic value about 0.54. This high proportion of final dissolved silica shows that Eq. (4) plays an important part in this experiment where initial hydroxide ions concentration is high. This proportion of final dissolved silica increases with the initial hydroxide ions concentration [23].

6.1.2. Evolution of n

The evolution of n according to time is given in Fig. 6. After a short plateau, which corresponds to n_0 ($n_0 \approx 0.07$), the content of Q_3 sites increases. For the studied aggregate, the mole fraction of Q_3 sites, n^* (Eq. (10)), at the end of the reaction is close to unity. This high content in Q_3 sites is characteristic of a silica gel formed by the hydroxylic breaking up of the siloxane bonds, probably following a topochemical mechanism.

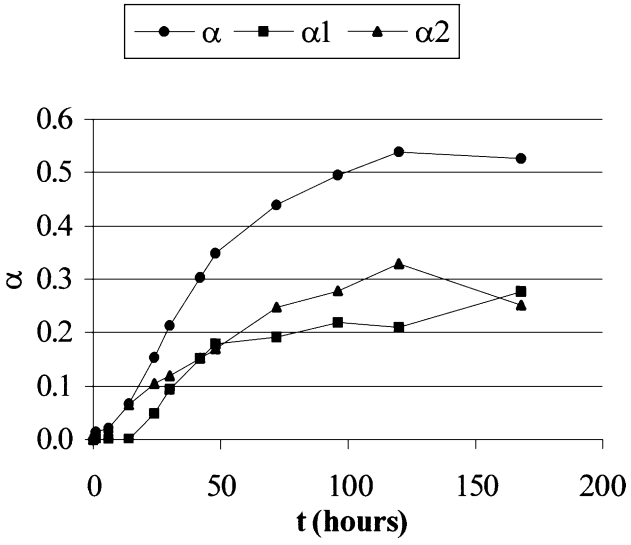

Fig. 5. Dissolution degree α as a function of time ($T = 80$ °C).

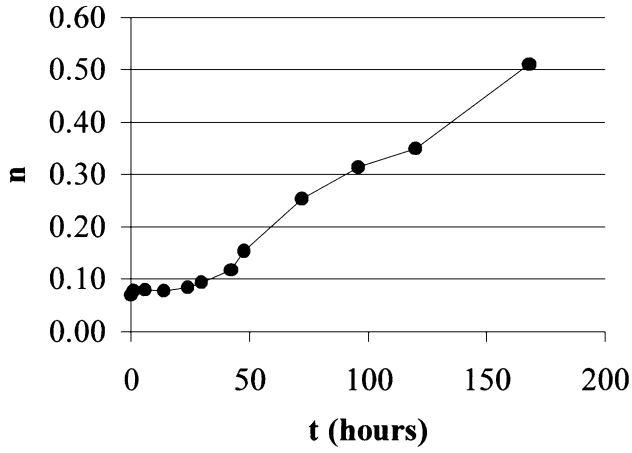

Fig. 6. Q_3 sites content n as a function of time ($T = 80$ °C).

6.1.3. Nature of the dissolved silica

The total dissolved silica corresponds to:

- free silica ions in solution and
- precipitated silica to form C-S-H and C-K-S-H.

To obtain the amount of free silica ions, we analyse the liquid phase filtered on 0.45-μm Millipore filters by ICP spectroscopy (Table 2). These solutions correspond to a saturated silica solution where the K^+ cations counterbalance the silica ions. We can define a specific reaction degree α_1 (Eq. (12)):

$$\alpha_1 = \frac{\text{moles of free silica ions}}{\text{moles of initial silica}} \quad (12)$$

Table 2
ICP analysis of the solution ($T = 80$ °C)

Reaction time (h)	Si (mol/l)	K (mol/l)	Ca (mol/l)
1	0.00	0.82	8.2e−04
6	0.00	0.81	7.6e−04
14	0.00	0.76	7.4e−04
24	0.08	0.74	2.4e−04
30	0.16	0.78	2.3e−04
42	0.25	0.78	2.0e−04
48	0.30	0.74	2.4e−04
72	0.32	0.68	1.9e−04
96	0.36	0.64	1.2e−04
120	0.35	0.60	7.6e−05
168	0.46	0.59	1.4e−04

Table 3
Proportions of silica species released in solution at 80 °C (quantitative results within ±10% uncertainty)

Reaction time (h)	Q_0	Q_1	Q_{2c}
2	0	0	0
18	1	0	0
54	0.60	0.25	0.15

The difference between total dissolved silica and free silica in solution determines precipitated silica α_2 (Eq. (13)) (Fig. 5):

$$\alpha_2 = \alpha - \alpha_1 \quad (13)$$

Up to $\alpha = 0.1$, the dissolved silica precipitates into C-S-H and/or C-K-S-H. Between 0.1 and 0.3, the dissolved silica increases while the precipitation continues. Over 30% of dissolution the solution is saturated in silica.

6.1.4. Characterisation of the silica ions in solution

Table 3 shows the proportion of free silica species in solution at different reaction times characterised by quantitative ^{29}Si NMR high-resolution spectroscopy. At the beginning of the reaction, the amount of silica in solution is too weak to be detectable. Soluble silica appears first in the Q_0 form. The Q_1 dimers and cyclic Q_{2c} species are formed next. These oligomers are probably produced by polymerisation of the monomers described by the Iler equilibria [24].

6.2. Relationship between n and α

The relationship between reaction degrees *n* and α (Fig. 7) evidences the competition between Step 1 and Step 2. For dissolution rates up to 0.3 approximately, the number of Q_3 sites increases slowly: The Q_3 sites formed following Eq. (1) are rapidly consumed by dissolution following Eq. (4). Afterwards, *n* increases with α: Step 1 forms more Q_3 sites than Step 2 can consume by dissolution.

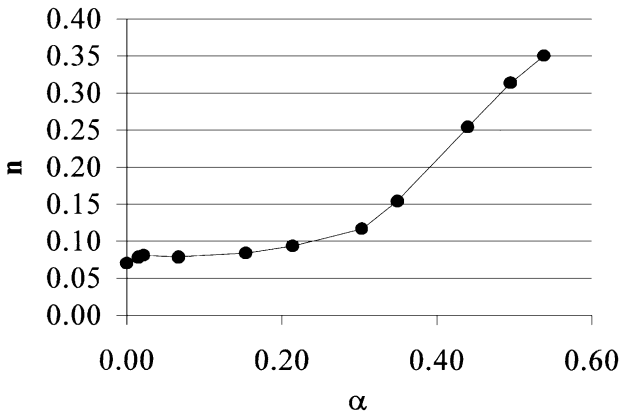

Fig. 7. Q_3 sites content *n* versus dissolution degree α ($T = 80$ °C).

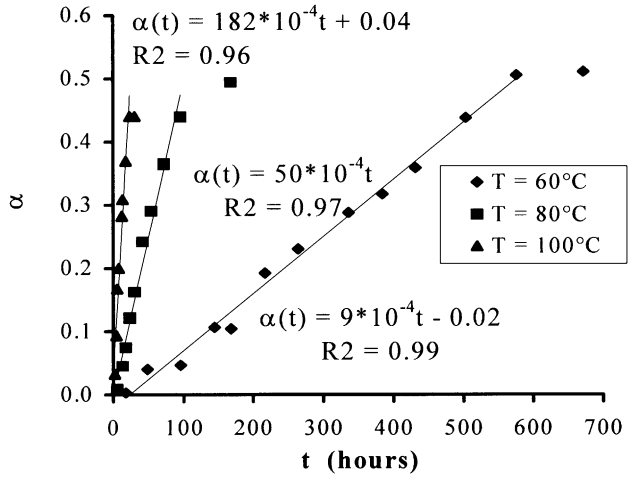

Fig. 8. Dissolution degree curves for three temperatures.

6.3. Temperature influence on reaction degrees

Figs. 8 and 9 represent the evolution of the dissolution degree α and the Q_3 sites content *n* for three temperatures: 60, 80 and 100 °C. In these experiments, the size distribution was [0–0.315 mm] and was not exactly the same as above [0.16–0.63 mm]. The other parameters are the same: 1 g of crushed aggregate, 0.5 g of $Ca(OH)_2$, 10 ml of a 0.79-M KOH solution. The [0–0.315 mm] size distribution contains 11% of fine particles, which, like a pozzolana, are immediately dissolved. Therefore, for the α and *n* calculations, we considered that initial aggregate quantity is not 1 g but 0.89 g. This does not affect the activation energy calculation.

6.3.1. The dissolution degree

The 60 and 80 °C curves (Fig. 8) present the same asymptotic value close to 0.5, and for the 100 °C curve, the

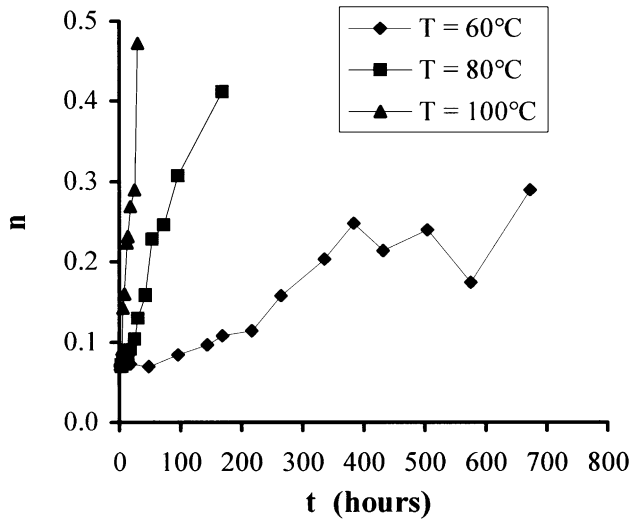

Fig. 9. Q_3 sites content curves for three temperatures.

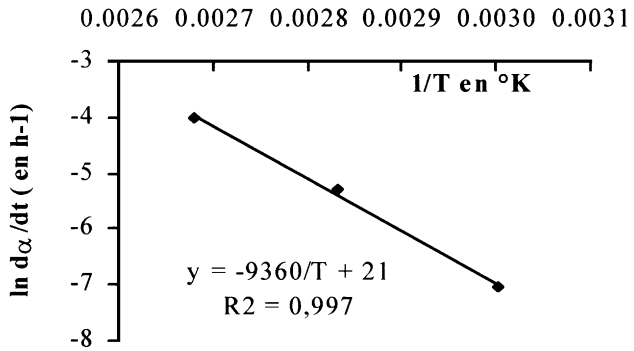

Fig. 10. ln(dα/d*t*) versus 1/*T*.

maximum dissolved ratio would be the same. The temperature has only a kinetic influence on the dissolution rate: the average rate $\Delta\alpha/\Delta t$ decreases with temperature. Using the Arrhenius law, we find an activation energy of 78 kJ mol^{-1} (Fig. 10). This value is close to the siloxane breaking up activation energy: The siloxane breaking up would be the limiting step of the dissolution process.

6.3.2. The Q_3 sites content

The asymptotic values for *n* at 60, 80 and 100 °C are not the same (Fig. 9): The maximum Q_3 site content decreases with temperature. This behaviour is probably related to the variations in solubility with temperature of the different silica species and also portlandite. It needs a further study.

6.4. Petrographic observations

Petrographic observations were carried out by H. Hornain and N. Rafai of LERM. Polished and thin sections were analysed using optical microscopy. Fig. 11 shows the initial particles. They show geometric shapes and uniform aspects, coming from the sizing of the aggregate. Fig. 12 presents altered aggregates for 14 h at pH 13.9 and 80 °C.

The sample is treated only by acid and is in the silanol form (State 2 in Fig. 4). The grains keep their geometric shape, but we can observe in some of them a growth of dark parts, which do not allow light transmission in thin section.

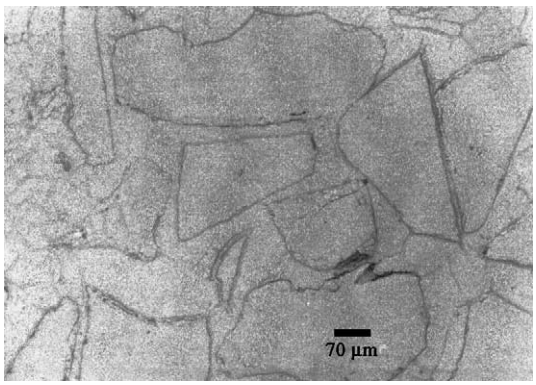

Fig. 11. Polished section of unreacted aggregates.

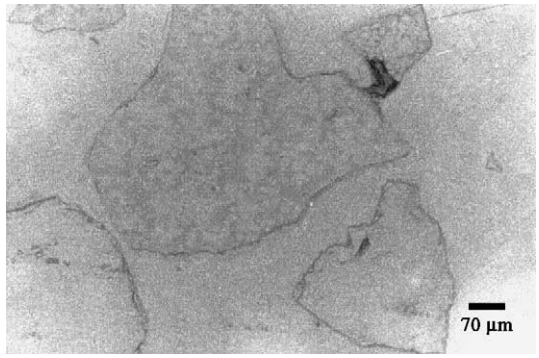

Fig. 12. Polished section of altered aggregates (14 h of reaction, $T = 80$ °C).

These petrographic investigations reveal the formation of an internal amorphous products formed by siloxane bonds breaking up. This chemical attack is due to KOH diffusion through the porosity of the aggregate.

7. Conclusion

This work develops a new chemical method for quantitative characterisation of ASR. The model reactor approach allows to quantify two reaction degrees, specific of ASR:

- *n* moles number of active Q_3 sites created by siloxane bond breaking up inside the aggregate and
- α moles number of monomers and small polymers obtained from Q_3 sites dissolution.

As ASR progresses, the formation of active sites prevails on dissolution and contributes to an internal silica gel formation. The limiting step is the siloxane breaking up.

Petrographic observations show that the reaction front penetrates deeply in the aggregate trough its connected porosity.

Using the same approach, the following topics will be discussed in further papers:

- the origin of the swelling, thanks to relationships between reaction degrees, aggregate porosity evolution and the dimensional change of mortars and
- the pessimum effect, thanks to relationships between reaction degrees and the hydroxide consumption for a high alkali and a low alkali medium.

Acknowledgments

This study received a financial support from "NORPAC" and "Ciments d'Obourg". We thank H. Hornain and N. Rafai of Laboratoire d'Etudes et de Recherche sur les Matériaux in Arles (France) for petrographic analyses.

References

[1] J.S. Guedon, F. Martineau, A. Le Roux, Visualisation des produits de l'alcali-réaction par fluorescence. Extension de la méthode au diagnostic sur ouvrage, Bull. Liaison Lab. Ponts Chaussees 179 (1992) 21–29.

[2] A. Leroux, Méthodes pétrographiques d'étude d'alcali-réaction, Bull. Geol. Ing. 44 (1991) 47–54.

[3] F.X. Deloye, L. Divet, The alkali–silica reaction: Quantitative considerations, Proceedings of the 9th International Conference on Alkali–Aggregate Reaction, London (England), Concr. Soc. Publ. CS 104 1, (1992) 251–260.

[4] The diagnosis of alkali–silica reaction, Report of a working party, British Cement Association publication, 1992, pp. 38–41.

[5] L.S. Dent Glasser, N. Kataoka, The chemistry of alkali–aggregate reaction, Proceedings of the 5th International Conference on Alkali–Aggregate Reaction, Cape Town (South Africa), National Building Research Institute of the CSIR, 1981, p. 7 (Paper S252/23).

[6] A.B. Poole, Alkali–silica reactivity mechanisms of gel formation and expansion, Proceedings of the 9th International Conference on Alkali–Aggregate Reaction, London (England), Concr. Soc. Publ. CS 104 1, (1992) 782–789.

[7] S. Urhan, Alkali silica and pozzolanic reactions in concrete: Part 1. Interpretation of published results and an hypothesis concerning the mechanism, Cem. Concr. Res. 17 (1987) 141–152.

[8] H. Wang, J.E. Gillot, Mechanism of alkali–silica reaction and significance of calcium hydroxide, Cem. Concr. Res. 21 (1991) 647–654.

[9] R. Dron, Thermodynamique de la réaction alcali–silice, Bull. Liaison Lab. Ponts Chaussees 166 (1990) 55–59.

[10] S. Chatterji, N. Thaulow, Some fundamental aspects of alkali silica reaction, in: M.A. Berube, et al. (Eds.), Proceedings of the 11th International Conference on Alkali–Aggregate Reaction in Concrete, Quebec (Canada), (2000) 21–29.

[11] S. Diamond, Alkali silica reaction — some paradoxes, in: A. Shayan (Ed.), Proceedings of the 10th International Conference on Alkali–Aggregate Reaction in Concrete, Melbourne (Australia), (1996) 3–14.

[12] R.A. Helmuth, D. Stark, Alkali silica reactivity mechanism, in: J. Skalni (Ed.), Materials Science of Concrete, vol. 3, American Ceramic Society, Westerville, OH, 1992, pp. 131–208.

[13] J. Lombardi, A. Perruchot, P. Massard, C. Larive, Study of Ca–Si gels products of alkali silica reaction: A comparison between hydraulic concretes and synthetic Ca–Si gels, in: A. Shayan (Ed.), Proceedings of the 10th International Conference on Alkali–Aggregate Reaction in Concrete, Melbourne (Australia), (1996) 934–941.

[14] A. Perruchot, P. Massard, J. Lombardi, Experimentation and volume variability of Ca–Si gels, first products of alkali silica reaction (ASR), in: M.A. Berube, et al. (Eds.), Proceedings of the 11th International Conference on Alkali–Aggregate Reaction in Concrete, Quebec (Canada), (2000) 81–87.

[15] S. Diamond, Chemistry and other characteristics of ASR gels, in: M.A. Berube, et al. (Eds.), Proceedings of the 11th International Conference on Alkali–Aggregate Reaction in Concrete, Quebec (Canada), (2000) 31–40.

[16] W. Wieker, C. Hubert, D. Heideman, R. Ebert, Alkali silica reaction — a problem of insufficient fundamental knowledge of the chemical base, in: M.D. Cohen, et al. (Eds.), Materials Science of Concrete: Special Volume — The Sidney Diamond Symposium, American Ceramic Society, Westerville, OH, 1998, pp. 395–408.

[17] W. Wieker, C. Hubert, D. Heideman, R. Ebert, Some experiences in chemical modelling of the alkali silica reaction, in: M.A. Berube, et al. (Eds.), Proceedings of the 11th International Conference on Alkali–Aggregate Reaction in Concrete, Quebec (Canada), (2000) 119–128.

[18] M.D.A. Thomas, The role of calcium in alkali–silica reaction, in: M.D. Cohen, et al. (Eds.), Materials Science of Concrete: Special Volume — The Sidney Diamond Symposium, American Ceramic Society, Westerville, OH, 1998, pp. 325–337.

[19] M. Kawamura, N. Arano, T. Terashima, Composition of ASR gels and expansion of mortars, in: M.D. Cohen, et al. (Eds.), Materials Science of Concrete: Special Volume — The Sidney Diamond Symposium, American Ceramic Society, Westerville, OH, 1998, pp. 261–276.

[20] M. Kawamura, N. Arano, K. Katafuta, ASR gel composition, secondary ettringite formation and expansion of mortars immersed in NaCl solution, in: M.A. Berube, et al. (Eds.), Proceedings of the 11th International Conference on Alkali–Aggregate Reaction in Concrete, Quebec (Canada), (2000) 199–208.

[21] AFNOR P18-589, Réactivité potentielle de type alcali silice et alcali silicate (test cinétique-méthode chimique), 1992.

[22] P. Longuet, F.X. Deloye, Exploitation des données apportées par l'analyse du béton durci, Annales de l'Institut Technique du Batiment et des Travaux Publics, Ser. Beton 216 (417) (1983) 30.

[23] D. Bulteel, E. Garcia-Diaz, J.M. Siwak, C. Vernet, H. Zanni, Alkali–aggregate reaction: A kinetic study, in: R.N. Swamy (Ed.), Proceedings of the International Conference on Infrastructure Regeneration and Rehabilitation: Improving the Quality of Life Through Better Construction — A Vision for the Next Millennium, Sheffield (England), (1999) 1041–1050.

[24] R.K. Iler, The chemistry of silica, Wiley, New York, 1979, p. 835.